Towards a complete census of active galactic nuclei in nearby galaxies : the incidence of growing black holes

A.D.Goulding, D.M.Alexander
B.D.Lehmer, J.R.Mullaney

2010MNRAS.406..597G

信田 和哉 (秋山研 : M1)

Table of contents

自己绍介!!

ABSTRACT

やったこと

- 近傍 (D < 15Mpc) の SMBH の密度関数と AGN に対する質量降着率の推定など
- 特に、$M_{BH} \simeq 10^{6\text{-}7} M_{sun}$ (あまりやられていない)
- [Ne V] を用いた AGN 判定
- Mass doubling time の推定
- etc. ...

INTRODUCTION

論文！…ちょっとその前に

NGC3621 (Opt & IR で AGN)

画像元:
http://sag2009.starspace.lv/public/ngc3621_aiz_lokalas_grupas_robezam_19092009.html;

AGN(Active Galactic Nuclei)

- 銀河中心の BH への質量降着によるポテンシャルエネルギーの解放により、明るく輝く現象

- 観測される大質量銀河は少なくとも 1 度は AGN による大規模な質量降着過程を経た!?

⇩

銀河と AGN の共進化

論文いんとろ Part 1

- Heckman et al(2004) (hereafter 『H04』)
  - SDSS のデータ
  - $\sigma > 70\mathrm{km/s} = M_{BH} \gtrsim 3\times10^{6}\ M_{sun}$
  - gas – rich であると optical は吸収が強くなってしまう
- resolution limit & Optical data という bias が掛かっている

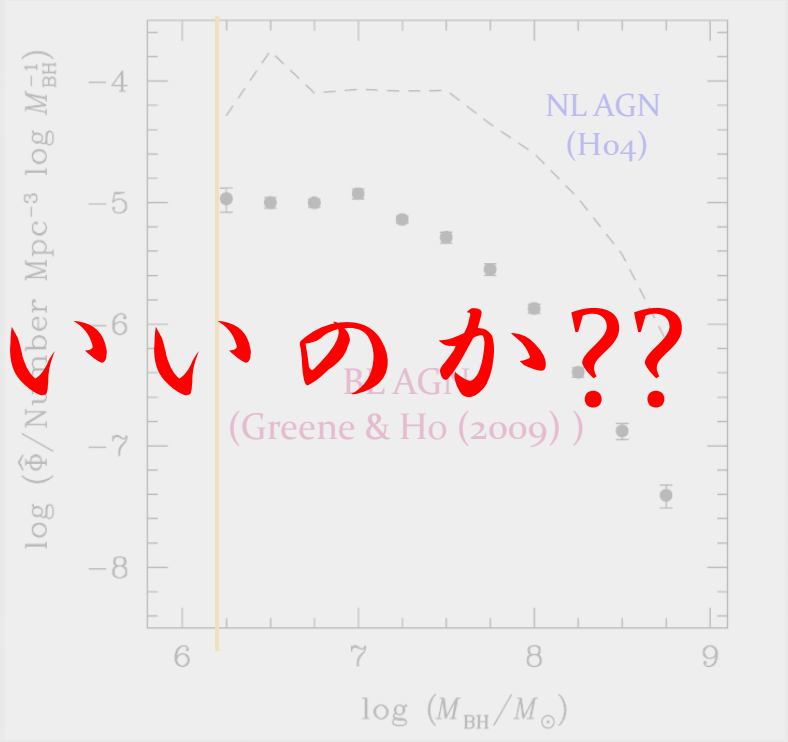

何を見たらいいのか??

Optical data のみだと、多くの AGN を見逃がしてしまう?!

論文いんとろ Part 2

Downsizing

high L_{AGN} ⇒ high-z

low L_{AGN} ⇒ low-z

昔の方が AGN はactiveで、より大きなBH が作られた!!

($M_{BH} \simeq 10^{8\text{-}9}\ M_{sun}$)

⇓ ということは…

近傍のactiveな AGN は $M_{BH} \ll 10^8\ M_{sun}$ ！

Low-z : $M_{BH} < 10^8\ M_{sun}$

Active : M_{BH} が大分小さい

Active

||

growth rate ($\dot{m}$ / M_{BH}) が高い

親論文

- A.D.Goulding
  & D.M.Alexander (2009)

  - 今回と同じサンプル
  - 50 % のAGN が optical のみだと見逃がされる
  - Mid-IR では Sc-Sd でも多い

後述

  - [Ne V] による AGN 同定
  - 見落とした 30% は starburst

結論

Late type spiral & dust rich
で見逃がされやすい!?

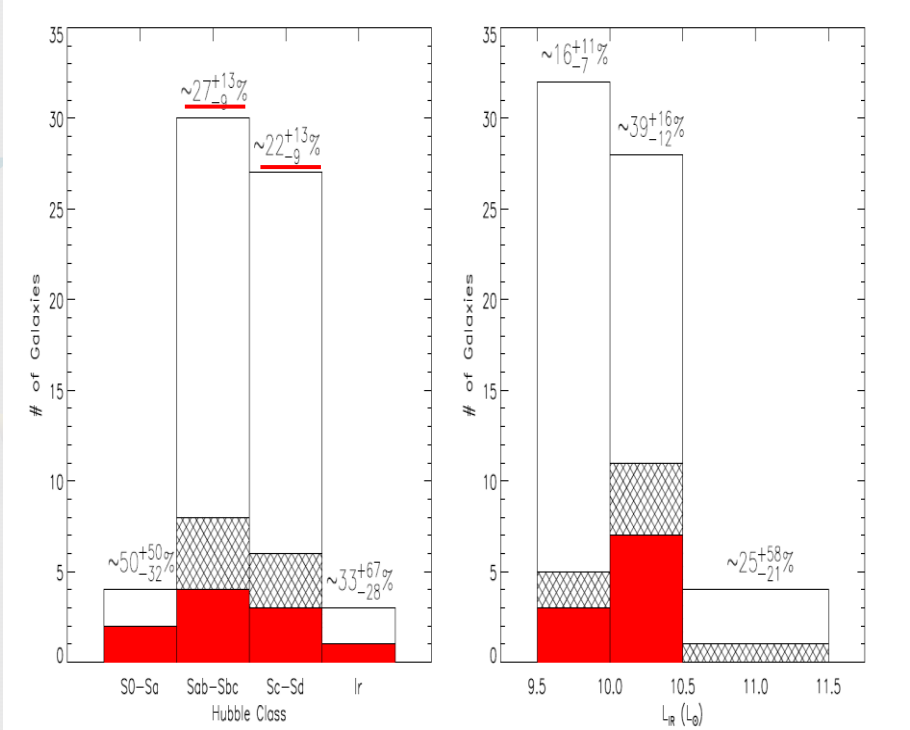

Figure 5. Fraction of AGNs identified in the $D < 15$ Mpc sample shown as a function of host-galaxy morphological classification and IR luminosity; the AGN fraction and associated 1σ errors are given for each sample bin. We further sub-divide the AGNs into [NeV] λ14.32 μm detected sources which are also optically observed to have AGN signatures (cross hatching), [NeV] λ14.32 μm detected sources which lack optical AGN signatures (solid colour), and combining these to give all galaxies with detected [NeV] λ14.32 μm emission, i.e. total number of AGN (cross-hatch+solid colour).

AGN が尻尾を隠して潜んでいる…

Optically unidentified AGN 10 コ

Host がダークレーンを持っていても Optical で同定されにくい

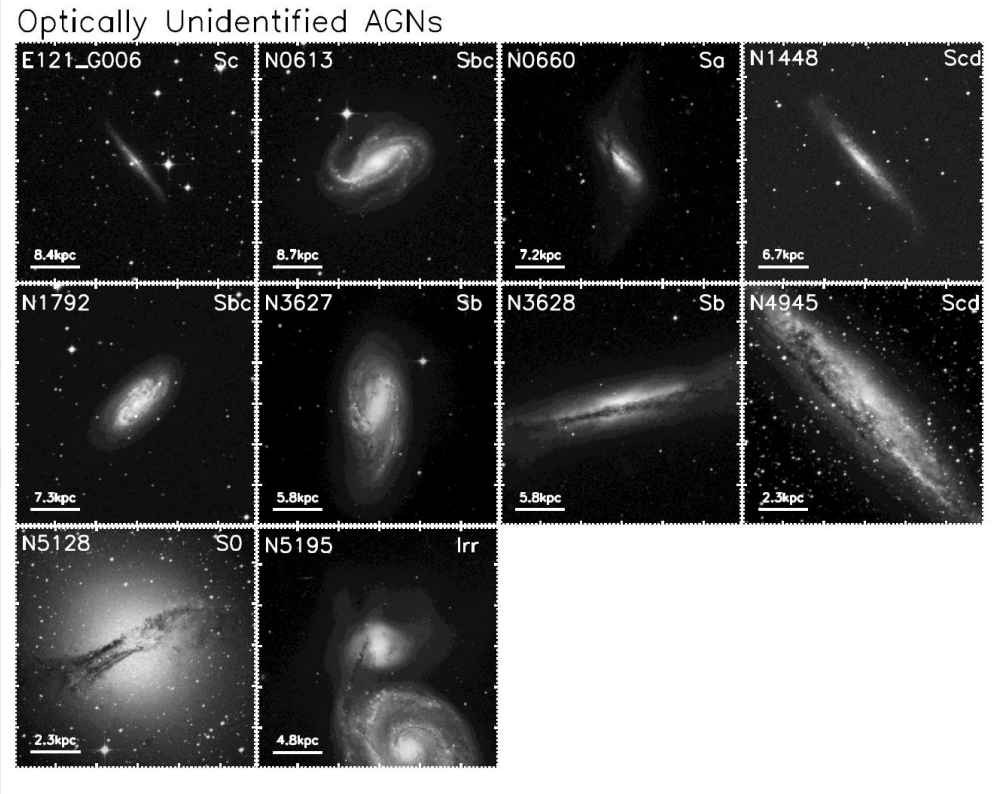

B&R band combined images
(Goulding & Alexander (2009))

いんとろ　まとめ

① Dust rich でも透過する波長
② 近傍の銀河
③ Late-type spiral & dust rich

Mid-IR & D < 15 Mpc,
late-type spiral & dusty
データでlow-mass M_{BH} について見てみよう！

SAMPLE

Galaxy Selection

- IRAS-RBGS

  (Revised Bright Galaxy sample)

  - 68 コ
  - D < 15 Mpc
  - $L_{IR} > 3 \times 10^9 L_{sun}$
    - Flux limit of RBGS

- Spitzer –IRS
  - high resolution データ
  - IRAS RBGS にもあるもの

➡ 64 コ のサンプル

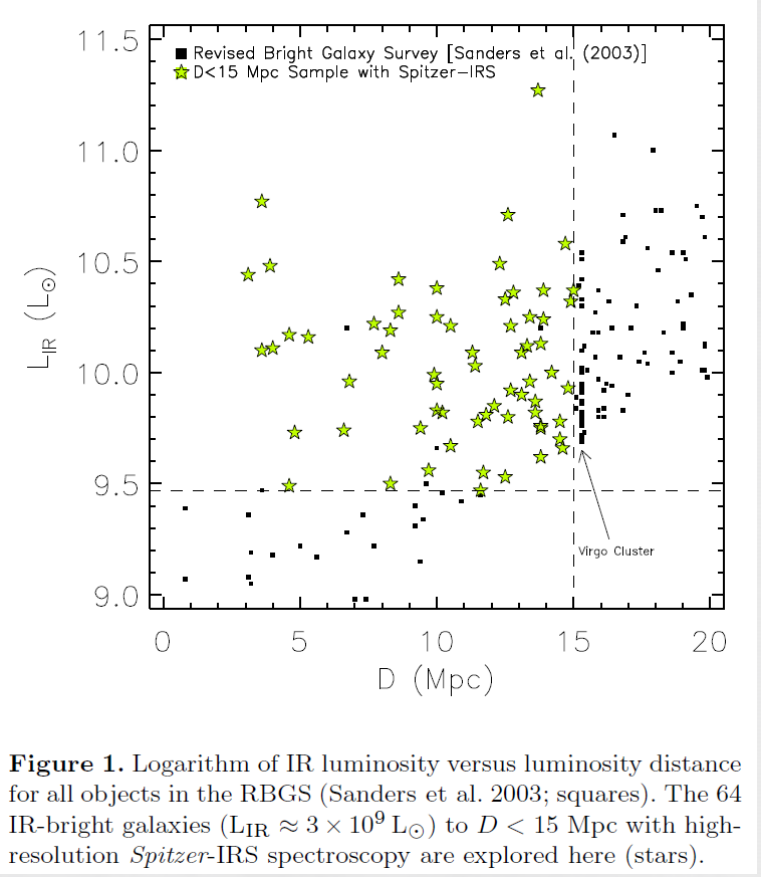

Figure 1. Logarithm of IR luminosity versus luminosity distance for all objects in the RBGS (Sanders et al. 2003; squares). The 64 IR-bright galaxies ($L_{IR} \approx 3 \times 10^9 L_\odot$) to $D < 15$ Mpc with high-resolution *Spitzer*-IRS spectroscopy are explored here (stars).

AGN Selection

- [Ne V] (λ14.32μm) による判定
  - 97.1 eV もの ionization potential

⇩

AGN くらいでないと観測されない

  - SMART(IDL) による fit

([Ne V] detection limit が不明...)

⇩

[Ne V] が同定された 17 コ で議論

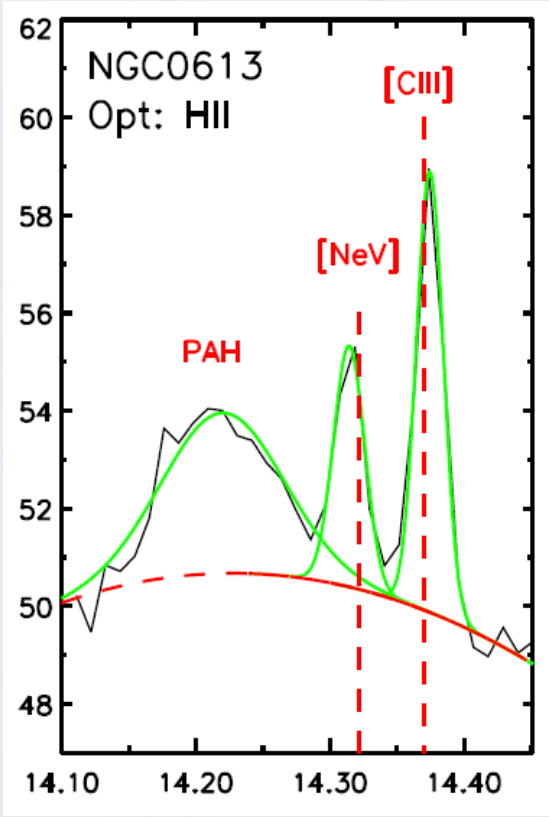

Line fit の様子 (GA09)

Sample list

割愛!!

Table 1. Catalogue of $D < 15$ Mpc mid-IR identified AGNs and derived quantities.

Common name (1)	D (Mpc) (2)	Hubble type (3)	AGN ID (4)	$\log(L_{[O\,IV]})$ (erg s^{-1}) (5)	$\log(L_X)$ (erg s^{-1}) (6)	Ref. L_X (7)	$\log(L_{bol,[O\,IV]})$ (erg s^{-1}) (8)	$\log(L_{bol,X})$ (erg s^{-1}) (9)	K_{Tot} (mag) (10)	K_{bul} (mag) (11)	$\log(M_{BH})$ ($M_\odot$) (12)	Method (13)	Ref. M_{BH} (14)
E121−G006	14.5	Sc	IR	39.04	–	–	41.82	–	8.98	10.91	$6.10^{+0.11}_{-0.51}$	L_{bul}	14
NGC 0613	15.0	Sbc	IR	39.38	–	–	42.26	–	7.03	–	$7.34^{+0.08}_{-0.15}$	M–σ_*	15
NGC 0660	12.3	Sa	IR	39.71	–	–	42.69	–	7.34	–	$7.35^{+0.08}_{-0.16}$	M–σ_*	21
NGC 1068	13.7	Sb	IR,O,X	41.66	43.48	1,9,2	45.26	44.85	5.79	–	$7.20^{+0.12}_{-0.12}$	M	16
NGC 1448	11.5	Scd	IR	39.40	–	–	42.28	–	7.66	10.64	$5.99^{+0.11}_{-0.52}$	L_{bul}	14
NGC 1792	12.5	Sbc	IR	38.26	–	–	40.49	–	7.01	9.08	$6.83^{+0.12}_{-0.53}$	L_{bul}	14
NGC 3621	6.6	Sd	IR,O	38.18	–	–	40.68	–	6.60	–	$6.50^{+0.13}_{-0.27}$	M–σ_*	22
NGC 3627	10.0	Sb	IR	38.38	–	–	40.95	–	5.99	–	$7.30^{+0.10}_{-0.19}$	M–σ_*	21
NGC 3628	10.0	Sb	IR	38.81	–	–	41.51	–	6.07	–	$6.53^{+0.07}_{-0.12}$	M–σ_*	20
NGC 4051	13.1	Sbc	IR,O,X	39.88	41.72	3,2,4,5	42.91	42.71	7.67	–	$6.15^{+0.16}_{-0.22}$	R	19
NGC 4945	3.9	Scd	IR,X	38.72	42.49	6,2,7,4,5	41.40	43.61	5.23	–	$6.04^{+0.05}_{-0.05}$	M	17
NGC 5033	13.8	Sc	IR,O,X	39.08	40.85	8,9	41.86	41.73	6.96	–	$7.62^{+0.09}_{-0.16}$	M–σ_*	21
NGC 5128	4.0	S0	IR,X,R[a]	39.38	41.85	2,9,4,5	42.26	42.86	3.94	–	$8.38^{+0.20}_{-0.26}$	G	18
NGC 5194	8.6	Sbc	IR,O,X	38.85	41.11	10,2	41.56	42.00	5.92	–	$6.88^{+0.13}_{-0.27}$	M–σ_*	15
NGC 5195	8.3	Irr	IR	37.89	–	–	40.30	–	6.25	–	$7.31^{+0.07}_{-0.13}$	M–σ_*	20
NGC 5643	13.9	Sc	IR,O,X	40.43	41.08	11,12,2	43.63	41.98	7.17	–	$6.44^{+0.11}_{-0.21}$	M–σ_*	23
NGC 6300	13.1	Sb	IR,O,X	39.78	41.63	13,4,5	42.79	42.60	6.93	–	$6.80^{+0.11}_{-0.22}$	M–σ_*	24

Note: (1) Common galaxy name. (2) Distance to source in Mpc from the Revised Bright Galaxy Survey (RBGS; Sanders et al. 2003). (3) Morphological type from RC3 (de Vaucouleurs et al. 1991). (4) Waveband of AGN identification; IR: mid-IR spectroscopy (GA09); O: optical spectroscopy (references presented in GA09); X: X-ray spectroscopy (2–10 keV; see column 7 for references); R: radio observations. (5) Logarithm of [O IV] λ25.89 μm luminosity in erg s^{-1} calculated using [O IV] flux presented in GA09; mean uncertainty is approximately 10 per cent. (6) Logarithm of absorption corrected hard X-ray luminosity (2–10 keV) in erg s^{-1} which have been converted to the distances given in column 2. (7) Reference for X-ray data. (8) Logarithm of bolometric luminosity of the AGN estimated from $L_{[O\,IV]}$ using equation (4). (9) Logarithm of bolometric luminosity of the AGN estimated from $L_{X,2-10\,keV}$ using the bolometric corrections described in Marconi et al. (2004). (10) Total K-band magnitude from 2MASS Large Galaxy Atlas (Jarrett et al. 2003). (11) K-band magnitude of bulge produced using GALFIT (Peng et al. 2002; see Section 3.2.1). (12) Logarithm of estimated black hole mass and associated 1σ errors in solar masses. (13) Method of M_{BH} measurement; M: maser mapping; G: gas kinematics; R: reverberation mapping; M–σ_*: mass–velocity dispersion correlation; L_{bul}: K-band luminosity–bulge correlation. (14) Reference for M_{BH} measurement.

References: (1) Matt et al. (1997); (2) Dadina (2007); (3) Pounds et al. (2004); (4) Tueller et al. (2008); (5) Winter et al. (2009); (6) Guainazzi et al. (2000); (7) Itoh et al. (2008); (8) Cappi et al. (2006); (9) Bird et al. (2007); (10) Fukazawa et al. (2001); (11) Maiolino et al. (1998); (12) Guainazzi et al. (2004); (13) Matsumoto et al. (2004); (14) this paper; (15) HyperLeda; (16) Greenhill et al. (1996); (17) Greenhill et al. (1997); (18) Marconi et al. (2001); (19) Wandel (1999); (20) Ho et al. (2009); (21) Barth, Ho & Sargent (2002); (22) Barth et al. (2009); (23) Whittle (1992); (24) Garcia-Rissmann et al. (2005).

[a]For a review see Israel (1998).

ANALYSIS PROCEDURE

必要なデータ

- M_{BH}
  - M_{BH} ごとの個数密度の推定
  - $L_{Edd} \propto M_{BH}$

- $L_{bol,AGN}$
  - Eddington ratio η
    - 推定された質量から得られる最大の光度

      (エディントン光度) と観測された全光度の比

$$\eta \sim L_{Bol,AGN}/L_{Edd}$$

M_{BH}

- 基本的に archival data を利用
  - Direct method (中心部の物理状態)
    - Reverberation mapping (1コ)
    - 水メーザー mapping (2コ)
    - 中心部のガスの kinematics (1コ)
  - Indirect method (環境から)
    - $M_{gal} - \sigma_*$ (10~11コ)

$$M_{BH} = (1.2 \pm 0.2) \times 10^8 M_\odot \left(\frac{\sigma_*}{200\,\mathrm{km\,s^{-1}}} \right)^{(3.75 \pm 0.30)} \quad (1)$$

Gebhardt et al.(2000)

    - $M_{BH} - L_{bulge}$ (3~4コ)

M_{BH} – L_{bulge} relation

- $L_{K,bulge}$ から推定
  1. GALFIT によるモデル化
  2. $L_{K,bulge}$ を決定
     - $L_{K,bulge}$ / $L_{K,disk}$
  3. Marconi & Hunt (2003)
     - M_{BH} - $L_{K,bulge}$

$$\log M_{\rm BH} = (8.08 \pm 0.10) + (1.21 \pm 0.13) \log\left(\frac{L_{K,\rm bul}}{8 \times 10^{10}}\right), \quad (3)$$

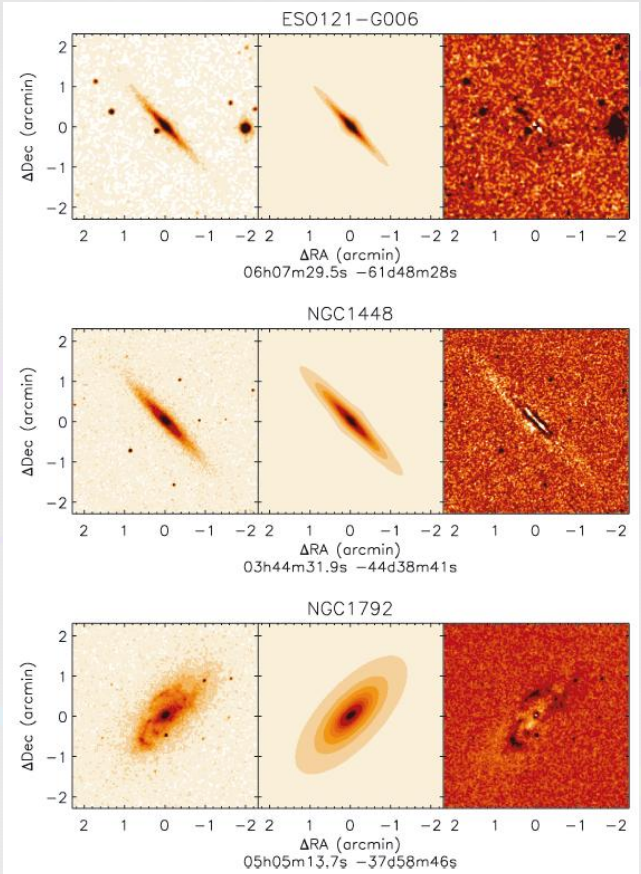

Figure 1. GALFIT (Peng et al. 2002) 2D bulge/disc decompositions for the three AGNs (ESO121−G006, NGC 1448 and 1792) with $M_{\rm BH}$ estimated from the $M_{\rm BH}$–$L_{K,\rm bul}$ relation. The panels show K-band 2MASS extended source image of the galaxy (left-hand part), GALFIT model produced by fitting a Sérsic profile, an exponential disc and a mean averaged background to the observed K-band image (middle part) and the residual image resulting from the subtraction of the model profile from the observed galaxy (i.e. observation − model) (right-hand part). See Section 3.2.1 for a brief explanation of the residual images.

$L_{bol,AGN}$

- 全波長データがあれば一番良い
  - ほとんど無理
- 透過し易い$L_{X\text{-}ray,2\text{-}10keV}$があれば大体補正可能

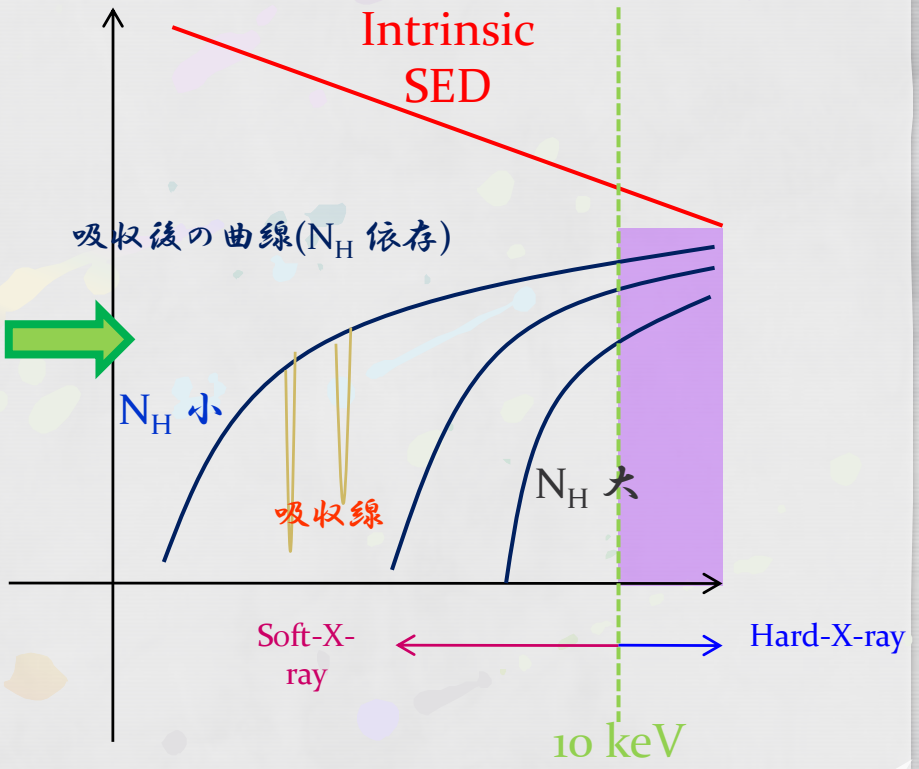

$L_{X\text{-}ray,2\text{-}10keV}$のデータが無いやつは??

$L_{X\text{-}ray(2\text{-}10keV)}$ - $L_{[OIV]}$

$L_{X\text{-}ray(2\text{-}10keV)}$ - $L_{[OIV]}$

⇩

??

- $L_{[OIV]}$ から推定
  - [OIV] はstar formation などからの影響が小さい
  - 透過率が大きい

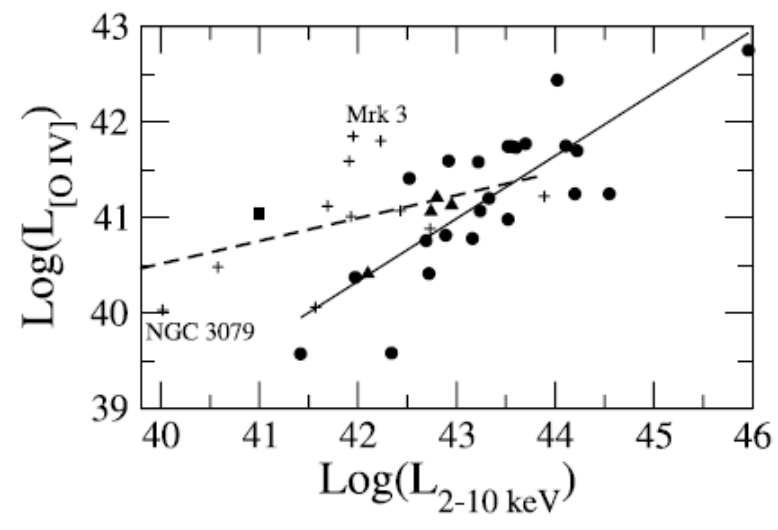

$$\log L_x = (0.4 \pm 0.1) \times \log L_{[OIV]} + (24 \pm 3).$$

Melendez et al.(2008)

さらなる変換

$L_{X\text{-}ray(2\text{-}10keV)} - L_{[OIV]}$

⇩

$L_{X\text{-}ray} - L_{bol,AGN}$

⇩

??

- Marconi et al.(2004)
  - $L_{X\text{-}ray} - L_{bol,AGN}$ relation

$$\log[L/L(2\text{–}10\,\mathrm{keV})] = 1.54 + 0.24\mathcal{L} + 0.012\mathcal{L}^2 - 0.0015\mathcal{L}^3,$$

where $\mathcal{L} = (\log L - 12)$ and L is the bolometric luminosity

$L_{bol} - L_{[OIV]}$

$L_{X\text{-}ray(2\text{-}10keV)} - L_{[OIV]}$

⇓

$L_{X\text{-}ray} - L_{bol,AGN}$

⇒ $L_{bol} - L_{[OIV]}$

- Dasyro et al(2008)
  - $L_{[O\,IV]} > 2 \times 10^{40}$ erg/s
  - 今回のサンプルを足すことで低光度側まで延長できた!!

$$\log\left(\frac{L_{bol,AGN}}{10^{44}\,\mathrm{erg\,s^{-1}}}\right) = (0.38 \pm 0.09) + (1.31 \pm 0.09)\log\left(\frac{L_{[O\,IV]}}{10^{41}\,\mathrm{erg\,s^{-1}}}\right) \quad (4)$$

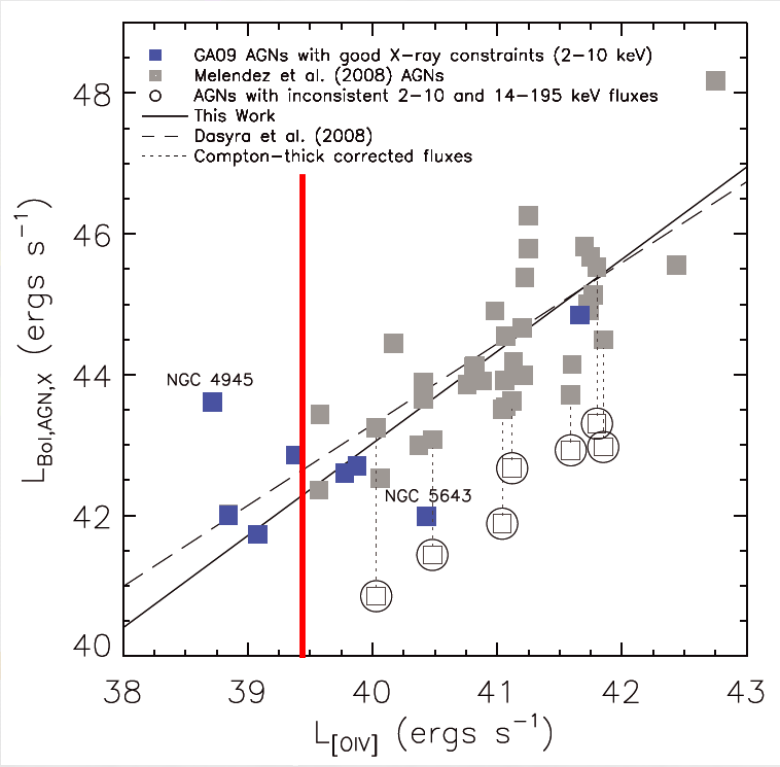

RESULTS & DISCUSSION

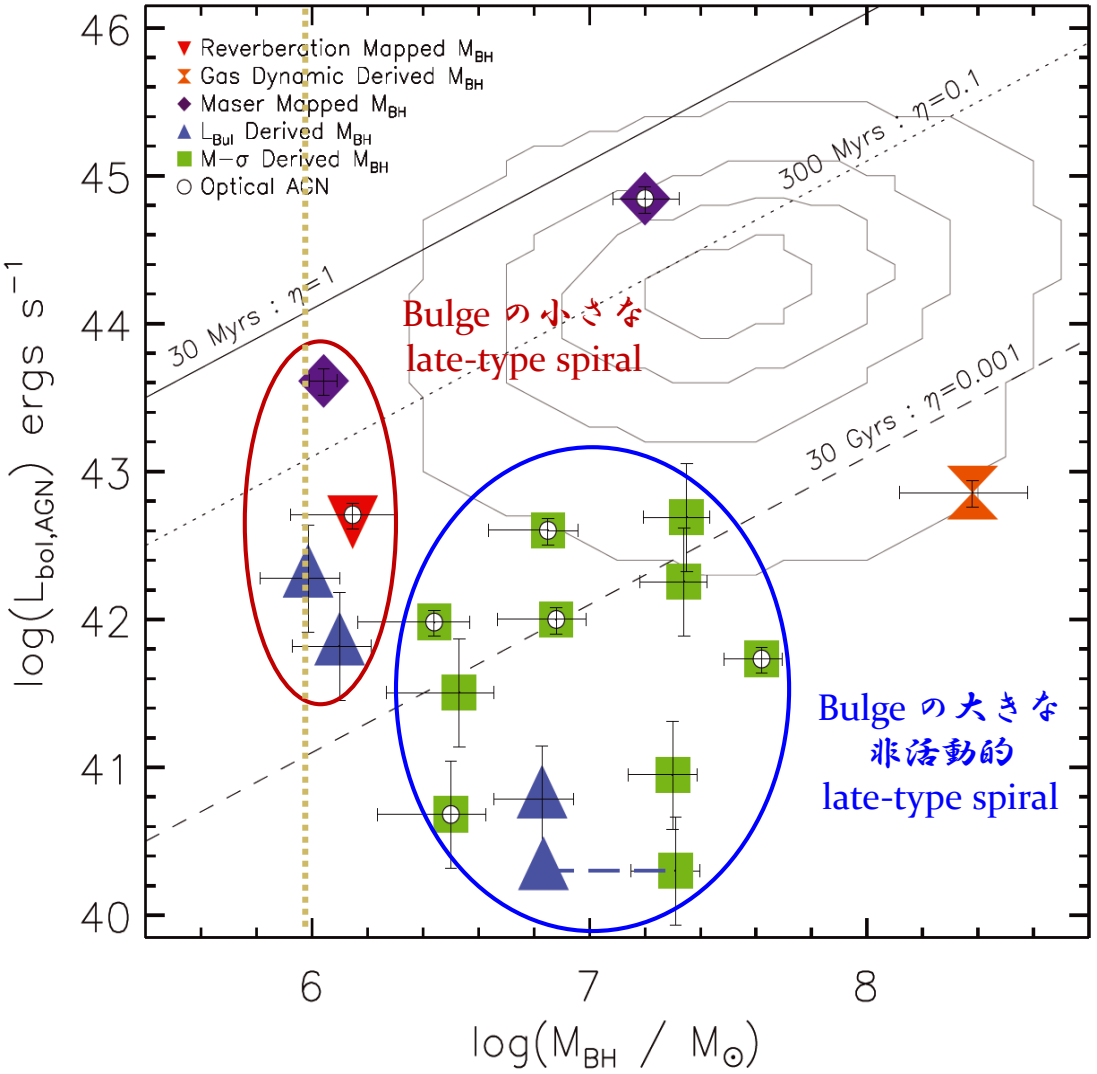

Figure 3. AGN bolometric luminosity ($L_{\rm Bol,AGN}$; in erg s^{-1}) is plotted against SMBH mass ($M_{\rm BH}$) for the $D < 15$ Mpc mid-IR identified AGNs presented in GA09. Associated 1σ error bars for $M_{\rm BH}$ and $L_{\rm Bol,AGN}$ estimations are shown (see Sections 3 and 5.1, respectively, for details of their derivations). AGNs which are previously identified in optical surveys are highlighted with open circles. AGNs with $M_{\rm BH}$ estimates from reverberation mapping (downward triangles), gas dynamics (hour glass), maser mapping (diamond), the M–σ_* relation (squares) and the $M_{\rm BH}$–$L_{K,\rm bul}$ relation (upward triangles) are plotted. NGC 5195 is represented with both an upward triangle and square (with a dashed-line connector) as both of the $M_{\rm BH}$ estimates for this galaxy are highly uncertain given its irregular morphology. Constant ratios of Eddington luminosity and their implied SMBH mass-doubling times are illustrated for $\eta = 10^{-3}, 10^{-1}, 1$ (30, 300 and 30 Myr; solid, short-dashed and long-dashed lines, respectively). Contours are shown for the active galaxies in the SDSS optical survey of H04. In general, we probe lower SMBH masses and AGN luminosities than those of H04, and we find that the majority of these AGNs would not be detected using optical SDSS data alone.

Figure 3.
M-L の関係

Eddington ratio とともに書いてあるのは、質量が2倍になるまでの時間

今回のサンプルは SDSS のデータに比べて、暗くて低質量なものが多い

$$\eta \sim L_{\rm Bol,AGN}/L_{\rm Edd}$$

Accretion ratio & properties of AGN

- $M_{BH} \simeq 10^6\, M_{sun}$ 付近の4コのうち、3コが Optical survey で同定されていない

  ⇒ Optical survey では多くの AGN を見逃がしている!?

- $M_{BH} \gtrsim 3\times10^6\, M_{sun}$ の Optically unidentified AGN は $\eta \lesssim 10^{-3}$ に多く分布

  ⇒ accretion があまり起こっていない or ADAF !?

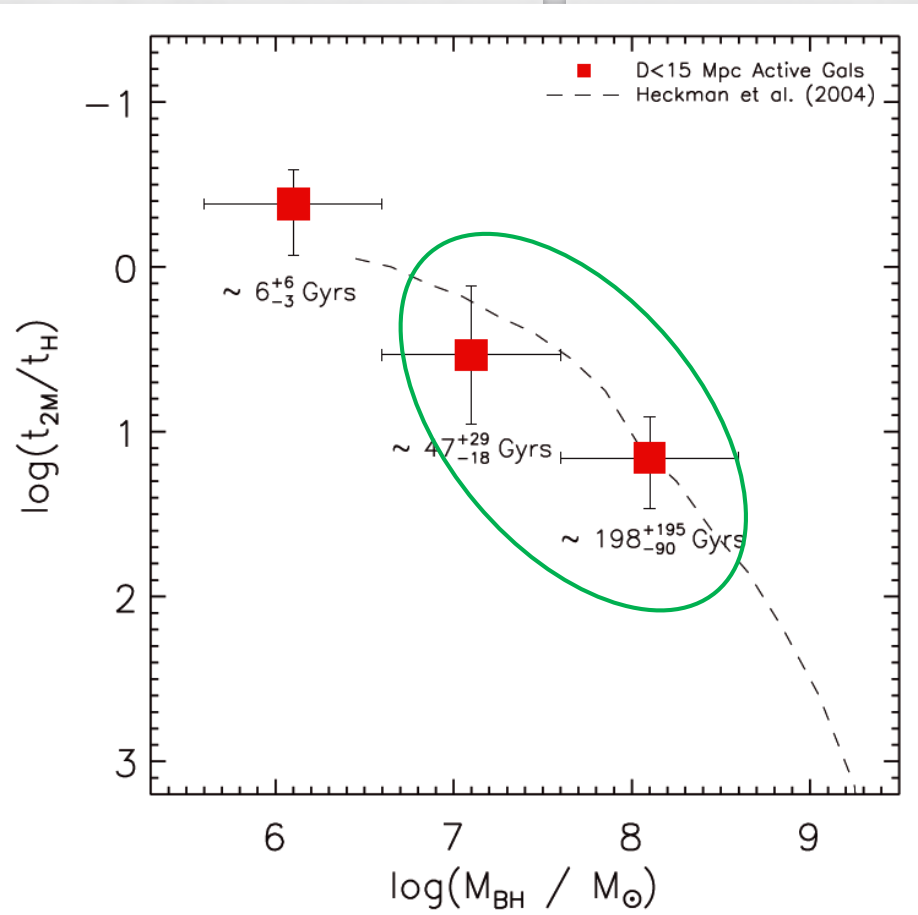

Figure 4. M_{BH} is plotted against the characteristic mean mass-doubling time (t_{2M}) of a SMBH in units of Hubble time (t_H) for the $D < 15$ Mpc AGNs. Growth time errors are calculated from the lognormal standard deviations of the sample. For comparison, the growth time function of H04 is shown (dashed line). We find good agreement with H04 over the region $M_{BH} \approx 0.3–10 \times 10^7\ M_\odot$ and further extend the growth time constraints to lower SMBH masses ($M_{BH} \approx 10^6\ M_\odot$).

Figure 4.
SMBH の活動性

今回のサンプルは H04 の関係を大体再現できている

$\Rightarrow M_{BH} \simeq 10^{7\text{-}8}\ M_{sun}$

現在最も成長しているのは

$M_{BH} \simeq 10^6\ M_{sun}$ くらいの AGN

大質量側はもう成長期を過ぎてしまっている…

Figure 5.

Volume average の個数密度

This work &
Optically identified
(dotted line)

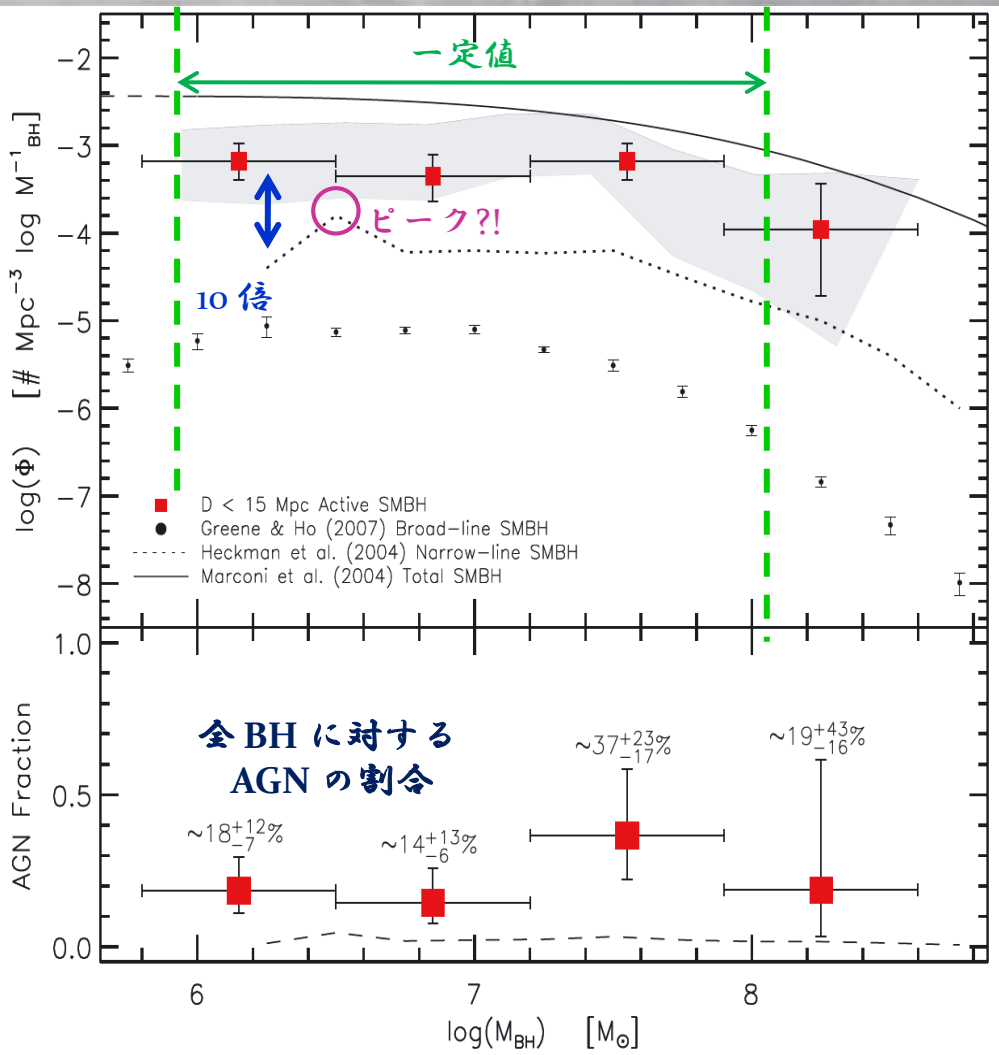

Figure 5. Upper panel: comparison of volume-weighted space densities of active SMBHs in the local Universe, Φ in units of number Mpc^{-3} log $M_{\rm BH}^{-1}$. Mid-IR active SMBH function (filled squares; GA09) is compared to the optically identified NL AGN function (dotted curve) of H04, the BL AGN function (filled circle) of Greene & Ho (2007), and total SMBH function (active + inactive galaxies; solid curve; Marconi et al. 2004). Sample selection bias is analysed using a robust Monte Carlo simulation (shaded region; see Appendix A). Lower panel: ratio of mid-IR active SMBHs to the total local SMBH mass function. The total SMBH mass function is extrapolated by 0.3 dex to $M_{\rm BH} < 10^6\,{\rm M}_\odot$. For comparison the volume-weighted AGN fraction of H04 is also shown (dashed line). We estimate a mean volume-weighted local AGN fraction of $\approx 25^{+29}_{-14}$ per cent over the range $M_{\rm BH} \approx (0.5\text{–}500) \times 10^6\,{\rm M}_\odot$.

Space density

- Optically AGN と Optically unidentified AGN
  - $M_{BH} \simeq (0.9\text{-}90) \times 10^6 M_{sun}$ では大体一定
  - Ho4 (SDSS) に比べて 10 倍大きい

  ⇒ 今回のサンプルのうち SDSS で同定されたのは

  2 / 17 ≃ 1 / 10 ⇒ consistent !!

  - さらに...今回の結果は lower limit

  ⇒ Palomar survey によると、少なくともあと4つの NL AGN が近傍には存在している(今回は luminosity limit などにより含まれていない)

Figure 5.

Volume average の個数密度

全質量範囲で考えると...

約 25 % に AGN が見られる

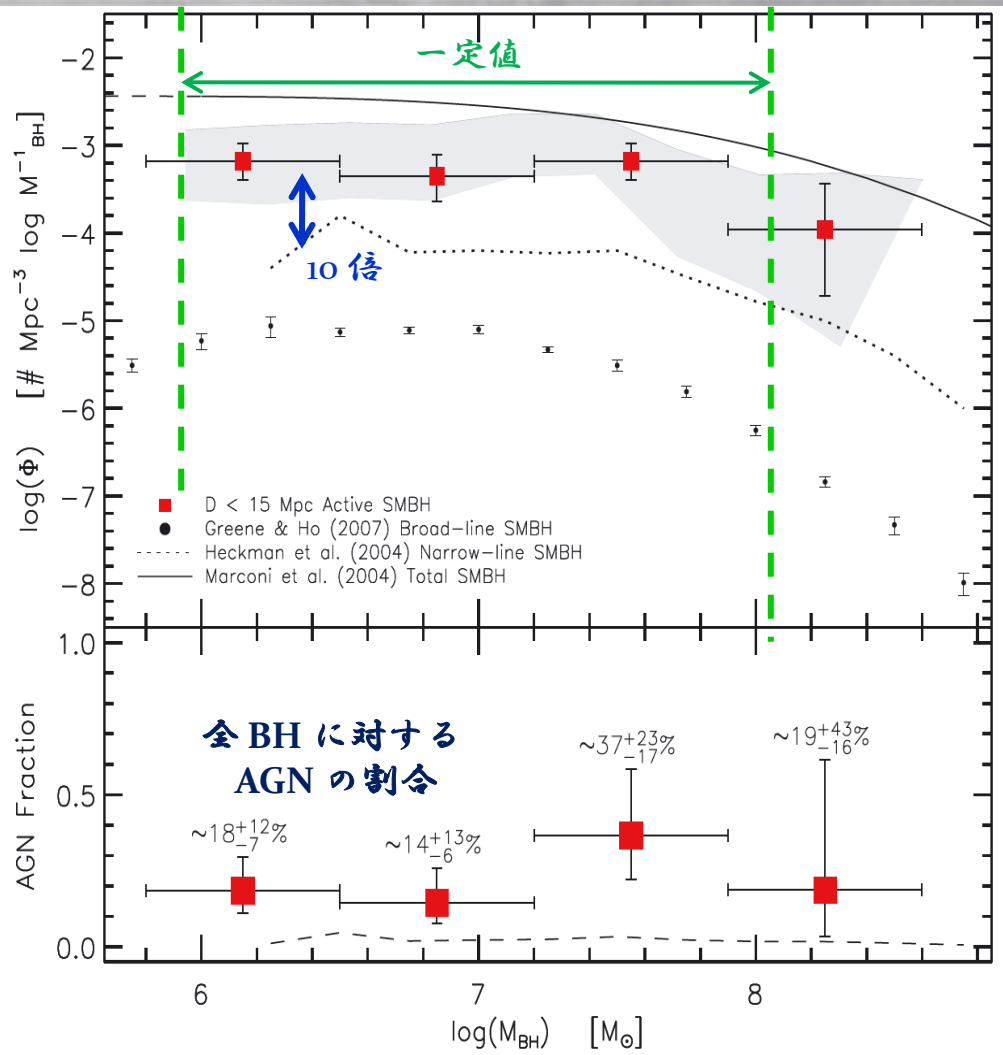

Figure 5. Upper panel: comparison of volume-weighted space densities of active SMBHs in the local Universe, Φ in units of number Mpc^{-3} log $M_{\rm BH}^{-1}$. Mid-IR active SMBH function (filled squares; GA09) is compared to the optically identified NL AGN function (dotted curve) of H04, the BL AGN function (filled circle) of Greene & Ho (2007), and total SMBH function (active + inactive galaxies; solid curve; Marconi et al. 2004). Sample selection bias is analysed using a robust Monte Carlo simulation (shaded region; see Appendix A). Lower panel: ratio of mid-IR active SMBHs to the total local SMBH mass function. The total SMBH mass function is extrapolated by 0.3 dex to $M_{\rm BH} < 10^6\,{\rm M}_\odot$. For comparison the volume-weighted AGN fraction of H04 is also shown (dashed line). We estimate a mean volume-weighted local AGN fraction of $\approx 25^{+29}_{-14}$ per cent over the range $M_{\rm BH} \approx (0.5\text{–}500) \times 10^6\,{\rm M}_\odot$.

AGN fraction

- 全 SMBH に対する AGN の割合
  - 約 25 % がAGN ($M_{BH} \simeq (0.5\text{-}500) \times 10^6\ M_{sun}$)
    ⇒ density が一定の部分で同様にfraction も一定値を示す
  - $M_{BH} \simeq (5\text{-}30) \times 10^5\ M_{sun}$ では約 18 % が AGN
    ⇒ small bulge galaxy の約 18 % が AGN であり、無視できるものではない
  - Eddington ratio を固定($\eta < 0.001$)して検証

    SMBH mass 減
    AGN fraction 増(8 ⇒ 16%)

    } Low mass の方が活発である という証拠

Space density

- Fig 3. (Fig 5.)について…
  - Ho4 や Greene & Ho (2007) では AGN fraction のピークは $M_{BH} \simeq 10^7\, M_{sun}$ だと推定

⇩

今回の結果を含めると $M_{BH} < 10^7\, M_{sun}$ では一定、
もしくは、増加しているようにさえ見える!!

⇩

さらに進める為には…

より多くの late-type spiral のデータが必要である

CONCLUSION

Main findingsPart 1

One

$M_{BH} \simeq 10^6\ M_{sun}$ では accretion rate は高い($\eta > 0.001$)ものの、 optical で同定できない AGN が多数存在している (Fig 3.)

Two

mass doubling time の推定(Fig 4.)

- $M_{BH} \simeq (0.5\text{-}50) \times 10^7\ M_{sun}$: $t_{2M} \simeq 47\text{-}198$ Gyr
  - Ho4 (SDSS) の結果と consistent
- $M_{BH} < 5 \times 10^6\ M_{sun}$: $t_{2M} \simeq 6$ Gyr
  - 現在最も活発に accretion が起こっている(rate が高い)

Main findings Part 2

Three

活動的 SMBH の space density function の延長(Fig 5.)

$M_{BH} \simeq 10^6 M_{sun}$ で SDSS の結果よりも少なくとも 2 倍は大きい値

$\Longrightarrow$ 無視できないほどの密度を持っている

Four

全 SMBH に占める AGN の割合

$M_{BH} \simeq$ (1-10)$\times 10^6 M_{sun}$: 約 25 % が AGN

Fin.